Journal of The Electrochemical Society, **157** (8) E117-E121 (2010)
0013-4651/2010/157(8)/E117/5/$28.00 © The Electrochemical Society

Direct Production of Ti–29Nb–13Ta–4.6Zr Biomedical Alloy from Oxide Mixture in Molten $CaCl_2$

Shogo Osaki,[z] Hiroshi Sakai, and Ryosuke O. Suzuki

Faculty of Engineering, Hokkaido University, Sapporo 060-8628, Japan

A process based on the principle of the Ono–Suzuki process involving electrolysis and the calciothermic coreduction of an oxide mixture consisting of TiO_2, Nb_2O_5, Ta_2O_5, and ZrO_2 for producing Ti–29Nb–23Ta–4.6Zr (TNTZ) was proposed. Ca was produced by the electrolysis of CaO in molten $CaCl_2$ by applying a voltage of 3.2 V between a carbon anode and Ti cathode at 1173 K. The residual oxygen concentration in the obtained powder decreased monotonically with an increase in the supplied electric charge. An oxygen concentration of 0.19 mass % was attained by supplying the electrical charge around 3 times larger than that necessary to generate the stoichiometrically required amount of Ca. This sample consisted of a Ti-based body-centered cubic solid solution and a small amount of hexagonal close-packed (hcp) solid solution. The inhomogeneity in the composition was suppressed to a relatively low level so that it could be easily improved by heat-treatment. After sintering at 1300 K for 54 ks, for example, the Ti- and Zr-rich hcp phase disappeared and the composition achieved the targeted value. The results of this study indicate that the OS process can be applied to directly produce TNTZ alloy from an oxide mixture.
 [DOI: 10.1149/1.3435302]

Manuscript submitted January 25, 2010; revised manuscript received April 26, 2010. Published June 3, 2010.

In recent years, new processes for producing Ti or Ti-based alloys have been investigated. The Ono–Suzuki (OS) process is one such process.[1-6] A schematic representation of the OS process is shown in Fig. 1. The OS process involves calciothermic reduction and Ca recycling. Ca is produced by the electrolysis of CaO in molten $CaCl_2$ electrolyte; Ca has a strong reducing capacity, and therefore, it can reduce various types of oxides. When a carbon anode and Ti cathode are used, the electrolysis reactions at the electrodes are expressed as follows

$$\text{At the anode:} \quad O^{2-} + C \rightarrow CO/CO_2 + e^- \qquad [1]$$

$$\text{At the cathode:} \quad Ca^{2+} + 2e^- \rightarrow Ca \qquad [2]$$

The overall reaction is expressed as follows

$$CaO + C \rightarrow Ca + CO/CO_2 \qquad [3]$$

The calciothermic reduction of a metal oxide (for example, TiO_2) is expressed as follows

$$TiO_2 + 2Ca \rightarrow Ti + 2CaO \qquad [4]$$

CaO that is formed as a by-product immediately dissolves in the molten $CaCl_2$, where CaO is electrolyzed again. These reactions permit the recycling of Ca used as a reducing agent and the continuous reduction of oxides in the same molten $CaCl_2$ bath.

Because of the wide solubility of CaO, the dissolution of O^{2-} from the oxide at the cathode was also studied as the direct electro-deoxidation,[7-10] which has been applied to TiO_2 using $CaCl_2$ melt especially applying a low electrochemical potential such as 2.0 V.

At a voltage higher than the theoretical decomposition voltage of CaO, the OS process has been successfully applied to the reduction of single oxides such as TiO_2 [1-6] and V_2O_5.[11] Recently, the principle of the OS process was applied to the synthesis of Ti–V–Cr hydrogen-storage alloy[12] and Ti–6Al–4V aerospace alloy.[13] In this study, we attempted to directly produce Ti–29Nb–13Ta–4.6Zr (TNTZ) alloy from an oxide mixture, as shown in Fig. 1.

TNTZ alloy is a newly developed alloy that is used for biomedical purposes and is expected to find wide-ranging applications because of its advantageous properties. Its constituent elements, namely Ti, Nb, Ta, and Zr, are nontoxic to biological bodies. In addition, it has a low Young's modulus of 60 GPa, much lower than that of pure Ti, which is beneficial in implant applications, and its mechanical strength is similar to that of Ti–6Al–4V alloy.[14] However, as is common in the case of Ti-based alloys, a method for producing TNTZ alloy remains complicated and expensive because the above-mentioned constituent elements need to be reduced individually before they are mixed. Furthermore, alloying methods such as arc melting require a considerable amount of electric power. If reduction and alloying could be carried out simultaneously, or more specifically, if the alloy could be directly produced from the oxide mixture, the production process could be considerably simplified; in fact, such an optimization might lead to TNTZ alloys finding wide-ranging applications.

The OS process could serve as this type of novel process for producing Ti-based alloys, because Ca can reduce most oxides and an alloy is synthesized simultaneously from the reduced metals during the process, as shown in Fig. 1, if some oxides are used as starting materials. In the production of TNTZ alloys, as shown in Fig. 2,[15] the constituent oxides can be reduced to their metallic phases by Ca because CaO is the most thermodynamically stable among the oxides shown in Fig. 2. Using an oxide mixture that consists of TiO_2, Nb_2O_5, Ta_2O_5, and ZrO_2 as the starting material, the individual oxides can be reduced simultaneously to form an alloy. The calciothermic coreduction of the oxide mixture is expressed as follows

$$TiO_2 + Nb_2O_5 + Ta_2O_5 + ZrO_2 + Ca \rightarrow TNTZ + CaO \qquad [5]$$

$$CaO + C \rightarrow Ca + CO/CO_2 \qquad [6]$$

In this study, we attempted to produce TNTZ alloy experimentally according to the reaction given in Eq. 5 and 6. The residual oxygen concentration and elemental distribution of the obtained sample were analyzed to confirm whether reduction and alloying proceeded successfully.

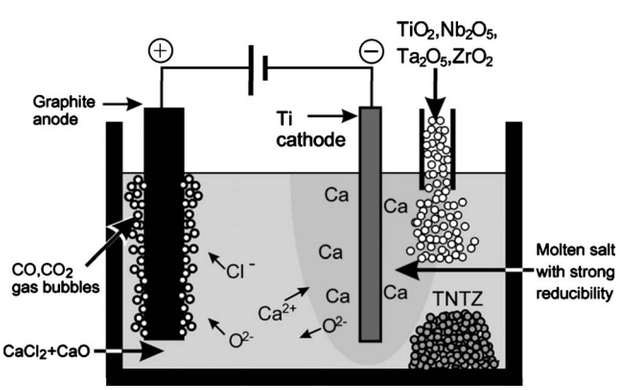

Figure 1. Principle of OS process for TNTZ alloy formation.

[z] E-mail: s.osaki@eng.hokudai.ac.jp

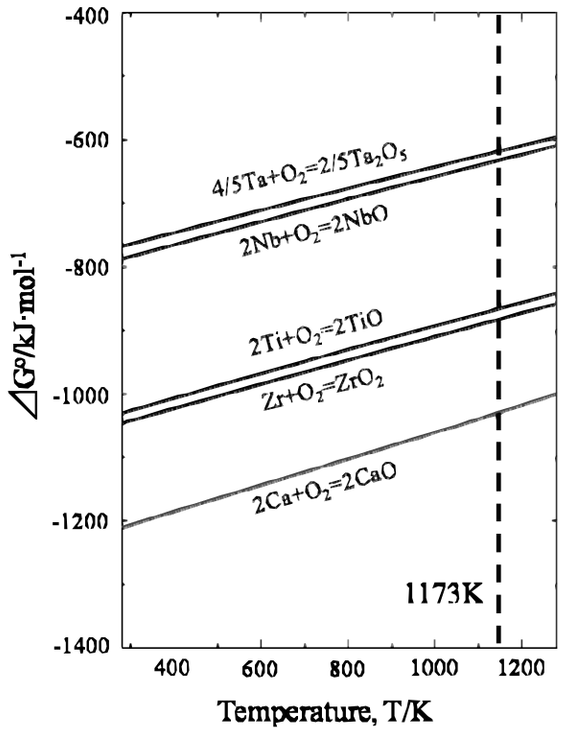

Figure 2. Oxygen partial pressure of the oxides in the system of Ti–Nb–Ta–Zr.

Experimental

Figure 3 shows the experimental apparatus used for carrying out the reduction of the oxide mixture and electrolysis. Molten $CaCl_2$ with 0.5 mol % CaO dissolved in it was used as the electrolyte. The mass of mixed salt was approximately 600 g. The anode was made of carbon and had a diameter of 10 mm, giving an active surface area of approximately 15 cm^2 when it was immersed in the molten salt. The cathode was made of Ti net and had a diameter of 12 mm; it had a cylindrical basketlike shape to hold the starting sample. The oxide powders, namely TiO_2, Nb_2O_5, Ta_2O_5, and ZrO_2, were weighted at the targeted composition with a mass ratio of TNTZ;

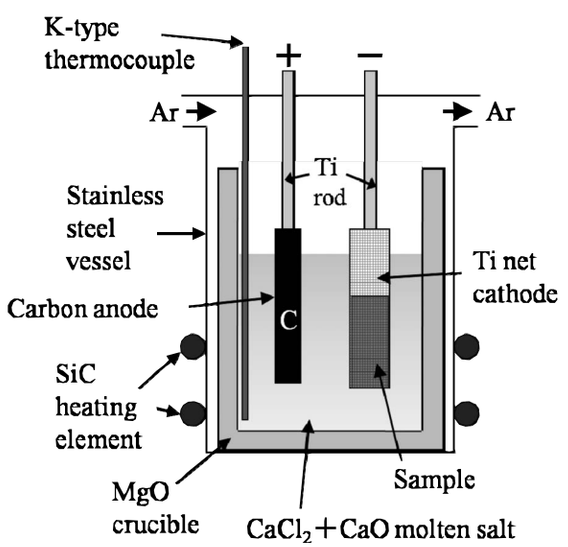

Figure 3. The experimental apparatus.

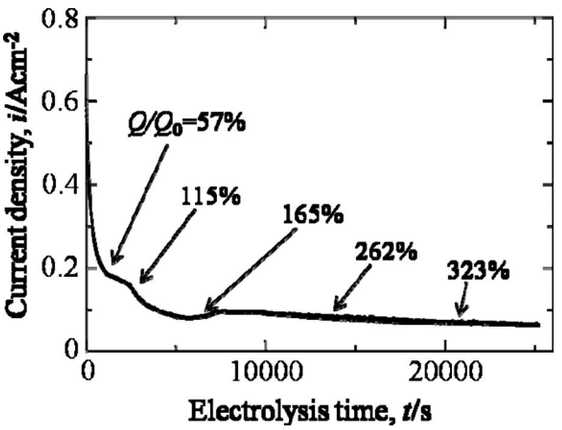

Figure 4. The change in anodic current density vs time.

they were then mixed thoroughly in mortar, before being inserted into the cathode. The mass of the starting oxide mixture was fixed at 2.00 g in all the experiments. The electrolysis vessel was evacuated at 873 K for approximately 30 ks to remove water present in the electrolyte.

Electrolysis was carried out under a constant potential of 3.2 V at 1173 K in Ar gas atmosphere. Q/Q_0 was used as an indicator to order the degree of reduction. Here, Q denotes the supplied charge and is calculated by integrating the measured current against time; Q_0 denotes the theoretical charge and is defined as the electricity required to generate a stoichiometric amount of Ca as given in Eq. 5. In this study, Q_0 was evaluated to be 8322 C.

After stopping electrolysis, the cathode was removed from the bath and cooled in Ar atmosphere. The reduced sample was sequentially washed with distilled water, acetic acid, ethanol, and acetone. It was then analyzed by X-ray diffractometry (XRD) and electron probe microanalysis (EPMA). The oxygen concentration of samples was also analyzed by using an IR absorption method with carbon crucible under He atmosphere using a LECO TC600 oxygen analyzer.

Several reduced samples were sintered for future application in powder metallurgy. The samples were pressed into a pellet (10 mm in diameter and thickness on the order of a few millimeters) at 450 MPa and then sintered in Ar atmosphere at 1300 K for 54 ks. The specimens were then analyzed by XRD and EPMA again.

Results and Discussion

Current density.— Figure 4 shows the change in anodic current density during electrolysis. The current exhibited a comparatively large value at the initial stage; it then gradually decreased and approached a low and constant value.

Under the assumption that the electrical carrier in molten $CaCl_2$ was mainly oxygen ions and the anodic reaction involves the evolution of CO and CO_2 gas, namely the consumption of oxygen ions, the large current would be attributable to the high reaction rate due to the high concentration of dissolved O^{2-}. The amount of O^{2-} decreased during the electrolysis, as indicated by Eq. 1, and the current due to O^{2-} decreased. In contrast, the amount of dissolved O^{2-} increased when reduction or deoxidation occurred effectively along with the generation of a large amount of CaO. Therefore, these changes in the dissolved O^{2-} are attributed to the current change.

After the complete reduction and removal of O^{2-}, the current should be zero. However, as shown in Fig. 4, a certain constant current continued to flow even at this final stage. This was due to the occurrence of parasite reactions in which Ca saturated in the molten salt reduced CO and CO_2 gas evolving at the anode.

Phases identified by XRD.— Figure 5 shows the XRD results of the reduced samples obtained at Q/Q_0 = 57, 115, 165, 262, and

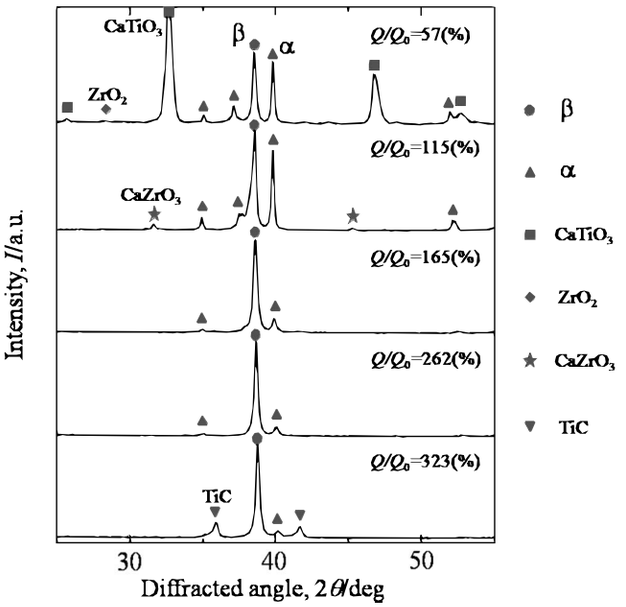

Figure 5. XRD patterns of reduced samples.

323%, as shown in Fig. 4. In Fig. 5, α and β correspond to hexagonal close-packed (hcp) and body-centered cubic (bcc) solid solutions, respectively.

At Q/Q_0 = 57%, α, β, $CaTiO_3$, and ZrO_2 were found. This indicates that the generation of Nb and Ta, which have a bcc structure, occurred effectively during electrolysis. However, TiO_2 would react with CaO dissolved in the molten salt to form the composite oxide $CaTiO_3$. ZrO_2 remained in the oxide form at this stage. This implies that the reduction behavior (reduction rate) could be classified into two groups, as predicted by the Ellingham diagram (Fig. 2). In other words, the free energy change in the chemical reaction (oxygen removal from the oxide) can be classified into two groups: a group of Ta and Nb, and another of Ti and Zr. The elements in the latter group are more stable than those in the former.

At Q/Q_0 = 115%, $CaTiO_3$ disappeared and $CaZrO_3$ was formed. In previous studies,[6,16] it was reported that $CaTiO_3$ was formed when the OS process reduced the TiO_2 starting material. In this study, it was confirmed that ZrO_2, whose metal has properties similar to those of Ti, also forms a composite oxide $CaZrO_3$. When the electric charge reached 165% of the theoretical value, only the α and β phases were found. Therefore, at this stage, all oxides might have been reduced to the metallic phase. At 262%, the XRD pattern obtained was similar to that obtained at 165%. The smaller intensity of the α peak indicated the transformation of α to β.

At 323%, TiC precipitation was observed. This is due to the generation of carbon via the reduction of CO and CO_2 as a parasite reaction or the direct reaction with Ti. To suppress TiC formation, the Ca-rich area should be separated from the anodic reaction area.

At all stages, a residual α phase was detected; in contrast, it was reported that the TNTZ alloy had a β single phase.[17]

Oxygen concentration.— Figure 6 shows the relationship between the residual oxygen concentration of the reduced sample and the supplied electric charge. The oxygen concentration decreased with an increase in the supplied electric charge, and it finally reached 0.23 mass % at Q/Q_0 = 262% (without TiC precipitation) and 0.19 mass % at Q/Q_0 = 323%.

A comparison of Fig. 6 with Fig. 5 indicated that the reduction completed before Q/Q_0 = 160%, following which deoxidation from the oxygen–metal solid solution proceeded. The α phase detected at Q/Q_0 = 115% included $CaZrO_3$.

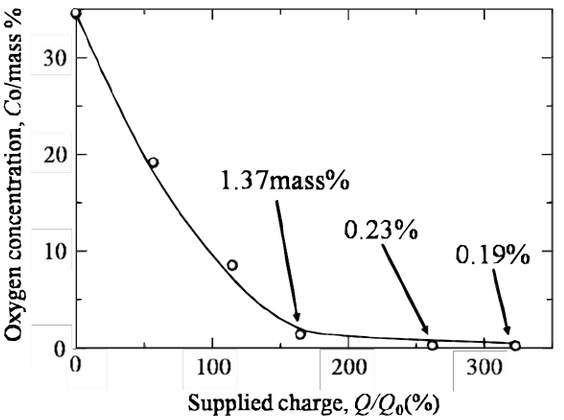

Figure 6. The change in oxygen concentration vs supplied charge.

Previously reported[18] arc-melted TNTZ alloys contained 0.05–0.15 mass % oxygen, and the increase in the oxygen concentration caused a larger mechanical strength that was offset by a smaller elongation. A TNTZ alloy including 0.1–0.7 mass % oxygen could be employed for a variety of applications.[19] Therefore, when producing TNTZ by our approach, it was concluded that the reduction and deoxidation proceeded sufficiently and the targeted residual oxygen concentration had been achieved.

Elemental distribution.— Figures 7-10 show scanning electron microscopic (SEM) images and the concentration mappings of the four elements in the reduced powders obtained for Q/Q_0 = 57, 115, 165, and 262%, respectively. In all figures, the brighter red color indicates a higher concentration.

At Q/Q_0 = 57%, most parts of the sample were in the form of fine particles having a diameter on the order of submicrometers. The constituent elements dispersed over the entire area; however, all were not present at the same location because alloying did not proceed sufficiently. At Q/Q_0 = 115%, it was clearly recognized that Nb and Ta existed at the same location. This implies that the alloying of Nb and Ta proceeded until this period. However, Ti existed more widely than Nb or Ta and some parts of α-Ti did not react with other elements. Zr localized at some parts, probably in the form of $CaZrO_3$. Figure 11 shows a magnified view of this sample. Table I lists the results of local elemental analyses carried out at the three positions shown in Fig. 11. Some rectangular blocks existed in this powder at locations that were rich in Nb and Ta. Therefore, this block was considered as a Nb–Ta-based bcc β-solid solution with

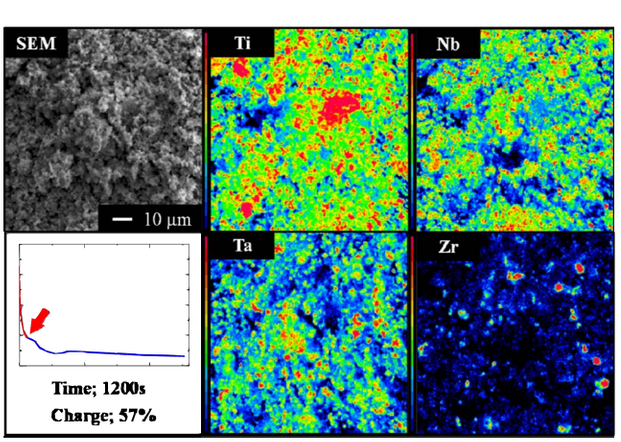

Figure 7. (Color online) SEM image and elemental concentration mappings of the sample obtained at Q/Q_0 = 57%.

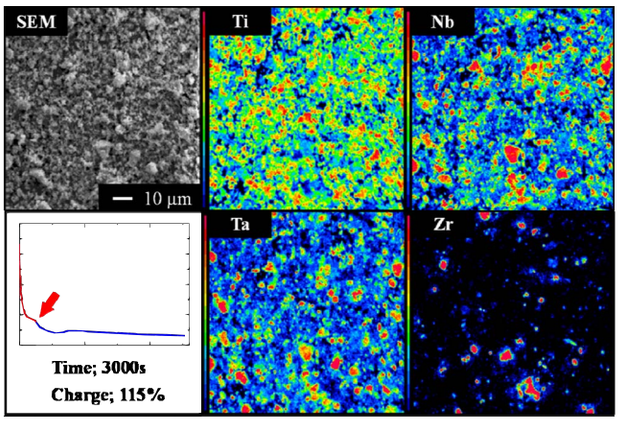

Figure 8. (Color online) SEM image and elemental concentration mappings of the sample obtained at Q/Q_0 = 115%.

19.2 mass % Ti. The fine particles marked as C are considered as α-Ti containing a larger amount of oxygen. Three types of elements coexisted, although the morphologies of the particles were dissimilar. The mixing of the constituent elements occurred at the oxide and alloy particle level, in addition to the individual reduction of elemental oxides. At Q/Q_0 = 165%, all of the constituent elements shown in Fig. 9 have spread more widely than those shown in Fig. 8.

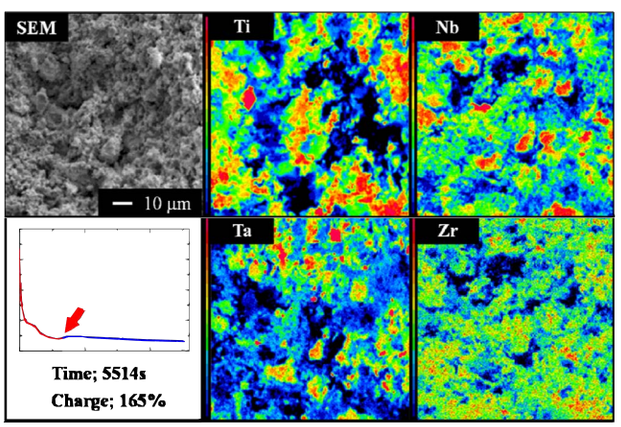

Figure 9. (Color online) SEM image and elemental concentration mappings of the sample obtained at Q/Q_0 = 165%.

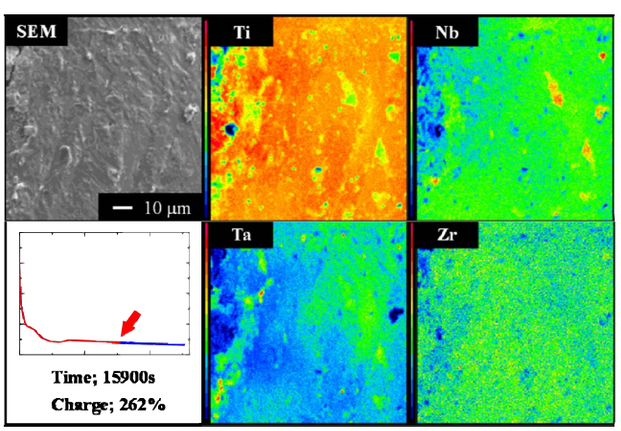

Figure 10. (Color online) SEM image and elemental concentration mappings of the sample obtained at Q/Q_0 = 262%.

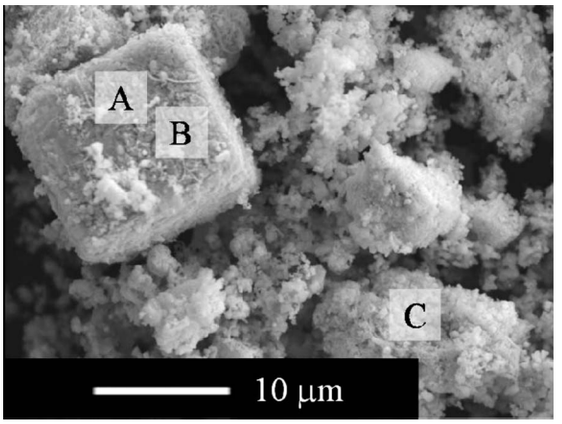

Figure 11. SEM image of the sample obtained at Q/Q_0 = 115%. The analytical values at A, B, and C are given in Table I.

All of the starting oxides including ZrO_2 were reduced to the metallic state at this stage and the sample formed secondary particles having a diameter of approximately 200 μm. At Q/Q_0 = 262% (Fig. 10), the elemental distribution became almost homogeneous, and the size of the secondary particles remained unchanged. Table II lists the results of local elemental analyses carried out at eight positions over the image shown in Fig. 10. This image was chosen at random and the spot size of a few micrometers was used. The deviations of the values listed in Table II are the standard deviation. Although Fig. 10 suggests that the four elements distributed homogeneously over a wide area, the measured compositions at eight locations exhibited slight variations.

This study showed that the reduction and deoxidation proceeded sufficiently and that the alloying proceeded simultaneously in molten $CaCl_2$. However, a residual α phase probably exists due to differences in the reduction behavior of the constituent oxides. The differences in the reduction rate lead to variations in the elements in the reduced powders. This is because the initial product Nb and Ta metals form blocks, whereas the delayed product Ti and Zr cannot

Table I. Local elemental analyses results at three positions in Fig. 11.

	Concentration (C/mass %)					
Position	Ti	Nb	Ta	Zr	Ca	O
A	19.2	51.2	21.4	0.2	0	8.0
B	19.2	50.5	21.6	0.4	0	8.3
C	31.5	37.0	21.1	0.5	0.1	9.8

Table II. Local elemental analyses results for the powder shown in Fig. 10.

	Concentration (C/mass %)			
Position	Ti	Nb	Ta	Zr
a	46.9	36.1	13.4	3.6
b	48.1	33.6	14.4	3.9
c	39.4	44.0	10.8	5.8
d	47.2	25.5	22.1	5.2
e	50.7	23.5	21.4	4.4
f	66.2	19.8	9.0	5.0
g	68.5	18.8	7.8	4.9
h	71.6	16.3	7.2	4.9
Average	54.8 ± 12.1	27.2 ± 9.8	13.3 ± 5.8	4.7 ± 0.7
TNTZ[14]	53.4	29	13	4.6

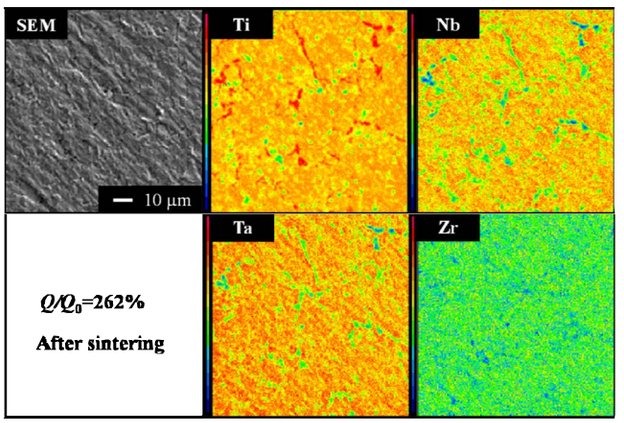

Figure 12. (Color online) SEM image and elemental concentration mappings of the pellet after sintering.

diffuse well into the blocks. Zr acts as an hcp stabilizing element in Ti alloy, whereas Nb and Ta act as bcc stabilizing elements.[20] Therefore, the variability of elements causes the residual α phase.

Improvement by heat-treatment.— From the viewpoint of future applications in powder metallurgy, we attempted to sinter the reduced powder to improve the compositional homogeneity. The powder obtained at Q/Q_0 = 262% was pressed into a pellet at 450 MPa and then sintered in Ar atmosphere at 1300 K for 54 ks. After cooling, the pellet was analyzed by XRD and EPMA.

The analytical results are shown in Fig. 12 and 13 and Table III. Figure 12 shows the SEM image and elemental distribution randomly selected in the sample, and Table III lists the analytical results at eight positions of this image. The compositional homogeneity was improved after the heat-treatment, and the analyzed compositions approached the targeted values with low variability. Figure 13 shows XRD patterns of the unsintered powder, sintered pellet, and solution-treated sample.[17] The sintered pellet had a β single phase and its XRD pattern agrees with that reported in a previous study.[17]

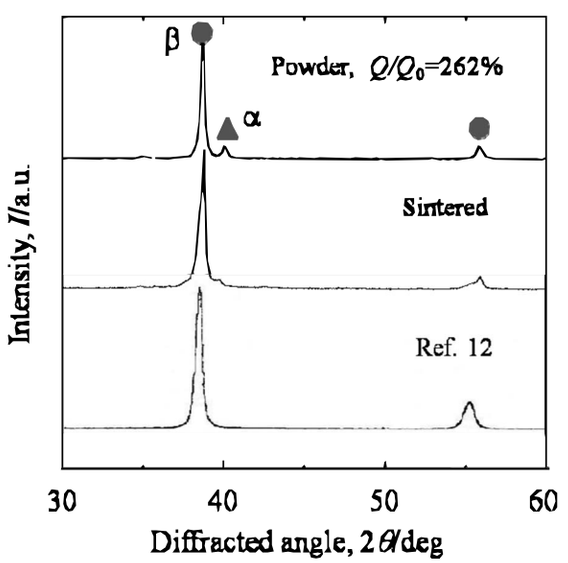

Figure 13. Comparison of XRD patterns.

Table III. Local elemental analyses results for the sintered pellet shown in Fig. 12.

	Concentration (C/mass %)			
Position	Ti	Nb	Ta	Zr
a	54.2	27.4	14.1	4.3
b	53.0	28.5	14.4	4.1
c	53.8	27.7	14.0	4.5
d	54.2	27.3	14.2	4.3
e	59.4	29.7	6.3	4.6
f	62.2	20.5	13.7	3.6
g	52.9	27.7	14.8	4.6
h	53.4	28.1	14.1	4.4
Average	55.4 ± 3.4	27.1 ± 2.8	13.2 ± 2.8	4.3 ± 0.3
TNTZ[14]	53.4	29	13	4.6

Conclusions

We proposed a process based on the principle of the OS process involving Ca coreduction and electrochemical recycling of Ca for producing Ti-based alloys. An oxide mixture consisting of TiO_2, Nb_2O_5, Ta_2O_5, and ZrO_2 was reduced simultaneously to form an alloy powder in molten $CaCl_2$. The oxygen concentration decreased monotonically with an increase in the supplied electric charge and reached 0.23 mass % without TiC contamination. The reduced sample with a low oxygen concentration was detected as a mixture of α and β phases, and its inhomogeneity was suppressed to a relatively low level although the reduction rates of the constituent oxides were different. The sample obtained after sintering had a β single phase with the targeted compositions. These facts indicate that the OS process can be applied to directly produce TNTZ alloy from an oxide mixture.

References

1. R. O. Suzuki and K. Ono, *Aqueous and Electrochemical Processing*, The Minerals, Metals & Materials Society, Warrendale, PA (2003).
2. R. O. Suzuki and S. Inoue, *Metall. Mater. Trans. B*, **34**, 277 (2003).
3. R. O. Suzuki, K. Teranuma, and K. Ono, *Metall. Mater. Trans. B*, **34**, 287 (2003).
4. K. Ono and R. O. Suzuki, *Materia Japan (Bulletin of The Japan Institute of Metals)*, **41**, 28 (2002).
5. R. O. Suzuki, *J. Phys. Chem. Solids*, **66**, 461 (2005).
6. R. O. Suzuki and S. Fukui, *Mater. Trans.*, **45**, 1665 (2004).
7. G. Z. Chen, D. J. Fray, and T. W. Farthing, *Nature (London)*, **407**, 361 (2000).
8. K. Dring, R. Dashwood, and D. Inman, *J. Electrochem. Soc.*, **152**, E104 (2005).
9. G. Z. Chen and D. J. Fray, *J. Electrochem. Soc.*, **149**, E455 (2002).
10. C. Schwandt and D. J. Fray, *Electrochim. Acta*, **51**, 66 (2005).
11. Y. Oka and R. O. Suzuki, *J. Jpn. Inst. Met.*, **72**, 181 (2008).
12. Y. Kano and R. O. Suzuki, *Ti-2007 Science and Technology*, The Japan Institute of Metals (2007).
13. H. Sakai, Y. Oka, and R. O. Suzuki, *J. Jpn. Inst. Met.*, **72**, 921 (2008).
14. D. Kuroda, M. Niinomi, H. Fukui, M. Morinaga, A. Suzuki, and J. Hasegawa, *Tetsu to Hagane*, **86**, 602 (2000).
15. A. Roine, HSC Chemistry, Version 6.1, Outotec Research Oy, Pori, Finland (2007).
16. K. Kobayashi, Y. Oka, and R. O. Suzuki, *J. Jpn. Inst. Met.*, **72**, 916 (2008); *Mater. Trans.*, **50**, 2704 (2009).
17. D. Kuroda, M. Niinomi, H. Fukui, A. Suzuki, and J. Hasegawa, *Tetsu to Hagane*, **86**, 610 (2000).
18. M. Nakai, M. Niinomi, T. Akahori, H. Ishikawa, and M. Ogawa, *J. Jpn. Inst. Met.*, **72**, 960 (2008).
19. F. Geng, M. Niinomi, M. Nakai, T. Akahori, and H. Tsutsumi, in *Proceedings of the Processing and Fabrication of Advanced Materials XVIII (PFAMXVIII)*, 176th Committee on Process Created Materials Function, Japan Society for the Promotion of Science, p. 1321 (2009).
20. H. Okamoto, *ASM Handbook*, p. 3, ASM International, OH (1992).